



## Large Magnetolectric Coupling in the Thin Film of Multiferroic CuO

Sudipta Goswami,\* Koushik Dey, Supriyo Chakraborty, Saurav Giri, Ujjal Chowdhury, and Dipten Bhattacharya

Cite This: <https://dx.doi.org/10.1021/acsomega.0c02211>

Read Online

ACCESS |



Metrics &amp; More

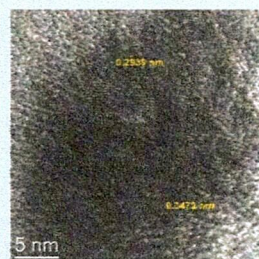


Article Recommendations

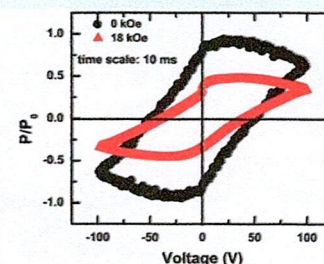


Supporting Information

**ABSTRACT:** We report observation of large magnetolectric coupling in an epitaxial thin film of multiferroic CuO grown on the (100)MgO substrate by the pulsed laser deposition technique. The film is characterized by X-ray diffraction, transmission electron microscopy, and Raman spectrometry. The crystallographic structure of the film turns out to be monoclinic (space group  $C2/c$ ) with  $[111]\text{CuO}||[100]\text{MgO}$  "out-of-plane" epitaxy and "in-plane" domain structure. The lattice misfit strain is found to vary within  $\pm 1\text{--}3\%$ . The dc resistivity, magnetization, dielectric spectroscopy, and remanent ferroelectric polarization have been measured across 80–300 K. The dielectric constant is found to decrease by  $>20\%$  under a moderate magnetic field of  $\sim 18$  kOe while the remanent ferroelectric polarization, emerging at the onset of magnetic transition ( $T_N \sim 175$  K), decreases by nearly 50% under  $\sim 18$  kOe field. These results could assume importance as the strain-free bulk CuO does not exhibit magnetolectric coupling within such magnetic field regime. The strain-induced large magnetolectric coupling in the CuO thin film would generate new possibility of further strain tuning to observe room-temperature magnetolectric multiferroicity suitable for scores of applications such as memories, sensors, energy-harvesting devices, generators, amplifiers, and so forth.



(a)



(b)

## 1. INTRODUCTION

The magnetolectric multiferroic systems, exhibiting coexisting ferroelectric and magnetic orders as well as a cross-coupling between the respective order parameters, are extremely attractive for a variety of future generation spintronics-based applications.<sup>1,2</sup> They range from four-state memories, sensors, spin-wave amplifiers, or magnetolectric generators to biomedical implants capable of correcting the gating action in damaged ion channels. However, for most of the applications as spintronic devices, large magnetolectric coupling is desirable at room temperature. Quite naturally,  $\text{BiFeO}_3$  has generated maximum interest because of its room-temperature multiferroicity.<sup>3</sup> Even then, large leakage current, volatility of Bi, and consequent formation of secondary phases during its synthesis, weak magnetolectric coupling under moderate magnetic or electric field raise doubts about its large scale practical usage. Alternative candidate systems such as  $\text{Bi}_5\text{Ti}_3\text{Fe}_{0.7}\text{Mn}_{0.3}\text{O}_{15}$ ,  $\text{Bi}_5\text{Ti}_3\text{Fe}_{0.7}\text{Co}_{0.3}\text{O}_{15}$ ,  $\text{Sr}_3\text{Co}_2\text{F}_{24}\text{O}_{41}$ , and so forth have indeed been discovered<sup>4</sup> during this period of renaissance in single-phase multiferroic systems since 2000. Ideally, a type-II multiferroic, where magnetism drives onset of ferroelectricity at or above room temperature, is the most suitable candidate.<sup>5</sup> This is because the change in the magnetic structure and/or anisotropy under externally applied magnetic field gives rise to enormous change in the ferroelectric polarization in such systems. Recent work<sup>6–9</sup> on CuO (tenorite) should have generated considerable interest, in

this context, because of its type-II multiferroicity at close to room temperature ( $\sim 230$  K). The incommensurate spiral magnetic structure breaks the inversion symmetry and drives onset of ferroelectricity at the magnetic transition temperature  $T_N$  ( $\sim 230$  K). From density functional theory and Monte-Carlo simulation, it has been shown that, under 20–40 GPa pressure, increase in the magnetic exchange coupling results in shifting of the  $T_N$  toward room temperature with more than three-fold increase in polarization.<sup>10</sup> Limited experimental support for pressure-driven room-temperature multiferroicity has also been received,<sup>11</sup> which, of course, was challenged subsequently.<sup>12</sup> However, in spite of coexistence of ferroelectric and magnetic orders, the magnetolectric coupling turns out to be poor<sup>13</sup> except at an extremely high field regime ( $\sim 500$  kOe) [ref 14]. This seems to have prevented generation of widespread interest in the multiferroicity of CuO. In this paper, we show, for the first time, that in a thin film of CuO, grown epitaxially on the (100)MgO substrate with  $[111]$ -axis perpendicular to the film surface, the magnetodielectric effect is substantial ( $>20\%$ ) even under a magnetic field of  $\sim 18$  kOe.

Received: May 12, 2020

Accepted: August 20, 2020



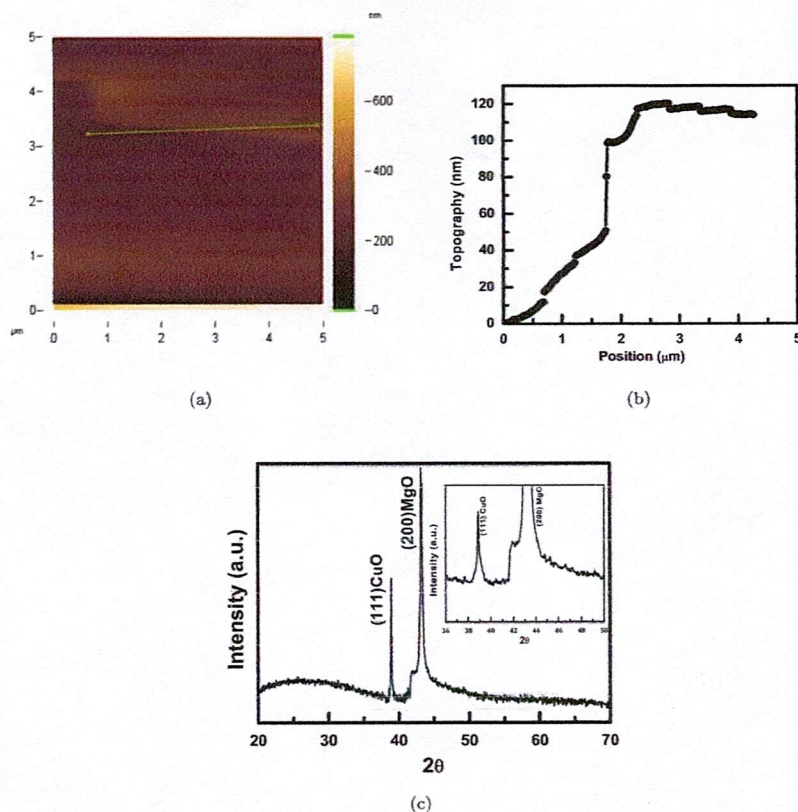


**Figure 1.** Representative (a) AFM topography image and (b) the line profile across the line shown in (a); (c) XRD  $\theta$ - $2\theta$  scan at room temperature across  $20$ – $70^\circ$ ; only (111) and (200) peaks could be observed from the film and substrate, respectively; no additional phase is present; the inset shows the blown-up peaks.

Finite remanent ferroelectric polarization is also found to emerge at  $T_N$ , which undergoes suppression by  $\sim 50\%$  under  $\sim 18$  kOe signifying the presence of strong magnetoelectric coupling.

## 2. RESULTS AND DISCUSSION

Figure 1a shows the representative atomic force microscopy (AFM) image recorded across a scratch, which exposes the film/substrate interface. The line profile across the scratch (Figure 1b) reveals the film thickness to be  $\sim 100$  nm. The average surface roughness of the film is found to be  $\sim 10$  nm. An additional line profile image and data collected across other parts of the film are shown in the Supporting Information. Figure 1c shows the result of  $\theta$ - $2\theta$  X-ray diffraction (XRD) scan recorded across a  $2\theta$  range ( $20$ – $70^\circ$ ). The (111) peak of CuO at  $2\theta = 38.8^\circ$  (JCPDS file 05-0661) could be observed close to the (200) peak of MgO signifying a high degree of out-of-plane epitaxy with  $[111]\text{CuO}||[100]\text{MgO}$ .<sup>15–18</sup> The low-angle shoulder around the (200) peak of MgO possibly results from oscillation in the diffraction intensity because of the Laue function term. The presence of peaks from other crystallographic planes could not be observed within this  $2\theta$  range. Also, no peak from the  $\text{Cu}_2\text{O}$  phase could be seen. Interestingly, although out-of-plane epitaxy (or, at least, a large scale texturing) is found to be present, in-plane epitaxy is lost. This has been observed by others as well for CuO thin films deposited on the (100)MgO substrate by both pulsed laser deposition and molecular beam epitaxy.<sup>15–18</sup> For instance, Catana et al.<sup>16</sup> shown from cross-sectional transmission

electron microscopy (TEM) that for films grown by pulsed laser deposition technique, the in-plane epitaxy is maintained only locally with three major epitaxial relationships  $[\bar{1}10]\text{CuO}||[110]\text{MgO}$ ,  $[0\bar{1}1]\text{CuO}||[110]\text{MgO}$ , and  $[10\bar{1}]\text{CuO}||[100]\text{MgO}$ . Similarly, molecular beam epitaxy technique too produces a film with out-of-plane  $[111]\text{CuO}||[100]\text{MgO}$  epitaxy yet in-plane polycrystallinity.<sup>15,18</sup> In the present case, we have used high-resolution TEM (HRTEM) rigorously to examine the in-plane crystallographic orientation of the film by capturing images from different edges of the film—primarily parallel to the film surface and away from the film/substrate interface. Figure 2a,d shows two representative HRTEM micrographs. More such images are available in the Supporting Information document. For more accurate determination of  $d$ -spacings of the lattice planes, first Fourier transformation (FFT) of the raw HRTEM image was generated, which was then inverted to yield clearer images of the lattice fringes. For instance, Figure 2b is the FFT of the selected region of Figure 2a. It shows two pairs of spots for two different planes,  $(\bar{1}12)$  and  $(112)$ . Figure 2c shows the corresponding lattice planes (generated from inverse FFT of Figure 2b), where  $(\bar{1}12)$  with  $d_{hkl} = 1.9590$  Å, and  $(112)$  with  $d_{hkl} = 1.7780$  Å. Similarly, selection from Figure 2d provides characteristic FFT [Figure 2e] with spots for  $(112)$  and  $(202)$ . Figure 2f shows the corresponding lattice planes, simulated (inverse FFT) from Figure 2e, where  $(112)$  with  $d_{hkl} = 1.7780$  Å and  $(202)$  with  $d_{hkl} = 1.8660$  Å. The presence of strain is clear, as shown in Figure 2d, as complex orientation is seen at regions where two (multiple) participating planes coexist at different orientations.



B

<https://dx.doi.org/10.1021/acsomega.0c02211>  
ACS Omega XXXX, XXX, XXX–XXX

*A. Radwan*  
Principal  
S.B.S.S. Mahavidyalaya, Goaltore  
Paschim Medinipur, Pin-721128